

# Modeling Steady-State Particle Size Spectra

ADRIAN B. BURD\* AND  
GEORGE A. JACKSON

Department of Oceanography, Texas A&M University,  
College Station, Texas 77843-3146

Fractal dimensions of marine aggregates are often estimated from the measured slopes of particle size spectra. One technique uses dimensional analysis to determine the dependence of the spectrum's slope with fractal dimension. In this paper, we use numerical simulations to examine the assumptions underlying the dimensional analysis approach to particle size spectra. We find that the slopes of numerically computed steady-state particle size spectra disagree with those predicted by dimensional analysis. The assumptions underlying the dimensional analysis approach that are responsible for the disagreement are as follows: only one coagulation mechanism operates in each particular particle size range, particle loss through sedimentation occurs at particle sizes larger than those for which differential sedimentation dominates, particles only interact with like-sized particles. Including disaggregation steepens the slope of the particle size spectrum for both large and small particles and changes the shape of the spectrum. These results indicate that one should exercise caution when using the measured slopes of particle size spectra to estimate aggregate fractal dimension.

## Introduction

Coagulation is an important process affecting the dynamics of particles in aquatic systems. It can control particle sedimentation in freshwater and oceanic environments (1, 2) and coagulation models and has been used to explain oceanic particle size spectra (3–5) as well as to describe the fate of algal blooms (7), trace metal scavenging (8, 9), and coagulation of metal oxides in aquatic systems (10, 11).

Coagulation models lead to the formulation of an equation (Smoluchowski's equation) for the evolution of the particle size spectrum that does not admit closed-form analytic solutions except under very special conditions (12). For other situations, solutions must be found using either suitable approximations or numerical methods. Two widely used and convenient approaches are the self-similar approximation and dimensional analysis.

Friedlander and co-workers (13–16) introduced and developed the self-similar approximation for solving the coagulation equation in order to explain the Junge spectrum found in atmospheric aerosols (see also ref 17). Such self-similar solutions are consistent with Smoluchowski's equation provided the coagulation rates satisfy certain homogeneity properties (18). They also agree well with numerical solutions for aerosols (19–21). However, aerosol research concentrates on particles  $< 1 \mu\text{m}$ , a size region where

Brownian coagulation dominates. Scaling theory has also been used to find solutions to the coagulation equation for fractal particles in aquatic systems (22).

Aggregation is known to lead to particles having a fractal, as opposed to solid, structure (23). In aquatic systems, particles range from colloidal (1 nm–1  $\mu\text{m}$ ) to the centimeter size range (24) where shear and differential sedimentation are the dominant mechanisms causing particle collisions. Wu and Friedlander have shown that for aerosols, low fractal dimensions increase the growth rate and lead to a broader particle size distribution (25); similar results were also observed for aggregation in aquatic systems in the numerical simulations of Burd and Jackson (26). Dimensional analysis arguments have been used to calculate size spectra for nonfractal marine particles (4, 27) as well as for fractal particles (5). These results have been used to estimate fractal dimensions of marine aggregates in a mesocosm (6).

Fractal dimensions of marine particles have been measured and range from 1.26 to 2.4 (28, 29). Jiang and Logan (5) estimated aggregate fractal dimensions using a dimensional analysis approach. The particle size spectrum in the steady state over a particular size range is assumed to be a power law function,  $n(r) \sim r^{\delta}$  (4, 5). For fractal particles, the calculated slopes are (5)

$$\delta_{\text{Br}} = -(1 + 0.5D) \quad (1)$$

$$\delta_{\text{sh}} = -(D + 5)/2 \quad (2)$$

$$\delta_{\text{ds}} = -\frac{1}{2} \left( 3 + D + \frac{2 + D - D_2}{2 - b} \right) \quad (3)$$

where  $D_2$  is a function of  $D$  and  $b$  is a function of the Reynolds number  $Re$ :  $D_2 = D$  if  $D < 2$ , otherwise  $D_2 = 2$ . For  $D = 3$ ,  $\delta_{\text{Br}}$  and  $\delta_{\text{sh}}$  are the same as those derived by Hunt for solid particles; for  $Re < 0.1$ ,  $\delta_{\text{ds}}$  is the same as that of Hunt (4) but for  $Re > 0.1$  is slightly smaller than Hunt's value.

The assumptions used in this approach include the following:

(i) The particle size distribution is in steady state, with source particles being created at a constant rate. Particles are removed from the system by sinking.

(ii) Only one mechanism (Brownian motion, shear and differential sedimentation, settling) operates at a given particle size range. For example, aggregation via Brownian motion dominates for particles of radius  $r_1$ ; shear for particles in the size range  $r_1 < r < r_2$ ; differential sedimentation for the size range  $r_2 < r < r_3$ ; only particles larger than  $r_3$  can settle out of the system. Implicit in this assumption is that particles coagulate with like-sized particles only.

(iii) The probability that two particles will adhere once they have collided (the sticking efficiency) is constant.

Not all of these assumptions necessarily hold. For example, under certain conditions, multiple aggregation processes can operate with similar rates for particles of a given size (2). An additional complication arises for particles that are large enough to sediment out of the system (17). The dimensional analysis approach does not incorporate the fact that sedimenting particles also coagulate by differential sedimentation.

The utility of the dimensional analysis approach is further compromised by not including disaggregation. Most particle size models for aerosols do not include particle breakup. Jackson and co-workers (24, 30) have shown that disaggregation is an important factor in predicting particle size spectra in marine systems. Analytical solutions of systems with only

\* Corresponding author phone: (979)845-1115; fax: (979)845-8219; e-mail: adrian@halodule.tamu.edu.

fragmentation have been shown to admit nonscaling solutions for homogeneous breakup kernels (31). As a result, the solutions may exhibit behavior that is not self-similar when disaggregation is included.

The aim of this paper is to examine some of the assumptions underlying the dimensional analysis approach to steady-state particle size spectra. We do this by comparing the slopes of the particle size spectrum calculated using eqs 1–3 with those obtained from numerical calculations for particles ranging from 1 μm to 1 mm in radius. We perform different numerical simulations by incorporating the assumptions i–iii listed above separately and together. We also examine the effects of a simple disaggregation model. Together, these results indicate that caution should be exercised when using a dimensional analysis approach to estimate fractal dimensions.

### Coagulation Model

The particle size spectrum,  $n(m, t)$ , is defined such that  $n(m, t) dm$  expresses the number concentration of particles in the mass interval  $m$  to  $m + dm$ . In the mean field theory, the evolution of  $n(m, t)$  in a well-mixed layer of thickness  $Z$  is determined from Smoluchowski's coagulation equation:

$$\frac{dn(m, t)}{dt} = \frac{1}{2} \int_0^m \alpha(m_1, m - m_1) \beta(m_1, m - m_1) n(m_1, t) \times n(m - m_1, t) dm_1 - n(m, t) \int_0^\infty \alpha(m, m_1) \beta(m, m_1) \times n(m_1, t) dm_1 - \frac{w(m)}{Z} n(m, t) + \phi(m) \quad (4)$$

where  $\beta(m, m_1)$  is the coagulation kernel for the collision between particles with masses  $m$  and  $m_1$ ,  $\alpha(m, m_1)$  is the probability that the two particles stick once they have collided,  $w(m)$  is the particle settling velocity, and  $\phi(m)$  the particle input rate (32).

We shall write the coagulation kernel as a sum of three terms as

$$\beta(m_1, m_2) = \beta_{Br}(m_1, m_2) + \beta_{sh}(m_1, m_2) + \beta_{ds}(m_1, m_2) \quad (5)$$

where the subscripts Br, sh, and ds refer to Brownian diffusion, shear, and differential sedimentation, respectively. This form implies that the coagulation mechanisms act independently (32).

For Brownian diffusion, the kernel for the collision between particles of radii  $r_i$  and  $r_j$  is given by

$$\beta_{Br}(r_i, r_j) = 4\pi(\mathcal{D}_i + \mathcal{D}_j)(r_i + r_j) \quad (6)$$

where  $\mathcal{D}_i = k_B T(6\pi\mu r_i)^{-1}$  is the diffusion coefficient for particle  $i$ ,  $k_B$  is Boltzmann's constant,  $T$  is the absolute temperature, and  $\mu$  is the dynamic viscosity of the fluid.

The kernels for shear and differential sedimentation involve an additional level of complexity: the inclusion of hydrodynamic forces. These forces are ignored in the rectilinear approximation which, for coagulation by shear, gives

$$\beta_{sh}(r_i, r_j) = (4/3)\gamma(r_i + r_j)^3 \quad (7)$$

where  $\gamma$  is the average shear gradient. For differential sedimentation, the rectilinear kernel is

$$\beta_{ds}(r_i, r_j) = \pi(r_i + r_j)^2 |w_j - w_i| \quad (8)$$

where  $w_i$  and  $w_j$  are the settling velocities of the particles  $i$  and  $j$  (e.g., ref 32).

In contrast to a solid body, there is no single, natural measure of the length of a porous aggregate. For a solid

sphere, the radius ( $r$ ) and volume ( $v$ ) are related by  $v = (4/3)\pi r^3$ . The irregular shape of an aggregate requires more than one length measurement to accurately characterize its shape. Alternatively, one can use an average measure of the aggregate size. The radius of gyration (or root mean square radius),  $r_g$ , is commonly used because it can be easily measured using photographic techniques. Another common measure is the radius of the equivalent volume sphere,  $r_v$  (i.e., the radius of the sphere having the same volume as the particulate material comprising the aggregate). The radius of gyration is used in this work unless stated otherwise. In previous work (26), we made use of the radius of the sphere that enclosed the aggregate volume. Our use of the radius of gyration in this work allows us to include some of the drag effects in the expression for the settling velocity.

As the solid mass of an aggregate is conserved in coagulation, we use it as the currency in our numerical simulations. Fractal scaling provides a relationship between particle mass and radius (33):

$$m = k r_g^D \quad (9)$$

where  $D$  is the fractal dimension and  $k$  is a constant. If the monomer particles are spheres of constant density  $\rho_0$  and radius  $a_0 = (3v/4\pi)^{1/3}$ , then  $k = (3/5)^{-D/2} (4/3)\pi\rho_0 a_0^{3-D}$ .

Particle settling velocity can be determined using a form of Stoke's law modified to allow for the fractal nature of the particles:

$$w = \frac{2g(\rho_0 - \rho_n)}{9\nu} r_v^3 r_g \quad (10)$$

where  $\rho_0$  is the density of the monomer particle,  $g$  is the acceleration due to gravity,  $\rho_n$  the density, and  $\nu$  is the kinematic viscosity of the water.

Various models for disaggregation have been proposed (34, 35). The formulation used here follows that of Jackson (30) where the breakup rate of particles in a section was given as being proportional to the rate in the previous, smaller section. For the  $k$ th section, this gives a breakup rate of

$$\text{breakup rate in } k\text{th section} = cb^k \quad (11)$$

The values of the constants  $c$  and  $b$  were taken from ref 30:  $c = 0.2$ ,  $b = 1.45$  for curvilinear kernels;  $c = 13.0$ ,  $b = 1.31$  for rectilinear kernels. The mass arising from particle breakup was spread uniformly over all sections smaller than that of the source particle. Results from this coagulation model have been previously compared with particle size spectra obtained from a mesocosm experiment (30).

Models of aggregate breakup can be quite involved (36–38). We have elected to use a far simpler model because of the many uncertainties that arise in using a more complex model. For example, marine aggregates are highly heterogeneous, containing dense fecal pellets, algal cells, and polysaccharide material. The size distribution of daughter particles resulting from the breakup of such an amalgam is presently unknown, as is the binding strength of material within the aggregate.

The numerical solution of eq 4 was obtained using the sectional approach (39, 7). All code was written in FORTRAN-77 and run on a DEC-Alpha 3000. The input rate,  $\phi(m)$ , was constant with time and taken to be non-zero only in the first section where it was constant. This input function simulated a monomeric source. The steady-state solutions,  $dn/dt = 0$ , were obtained using a globally convergent Newton's method for nonlinear systems (40). When disaggregation was included, this numerical scheme occasionally resulted in negative particle concentrations. When this happened, we integrated the system using a Bader–Deuffhard algorithm

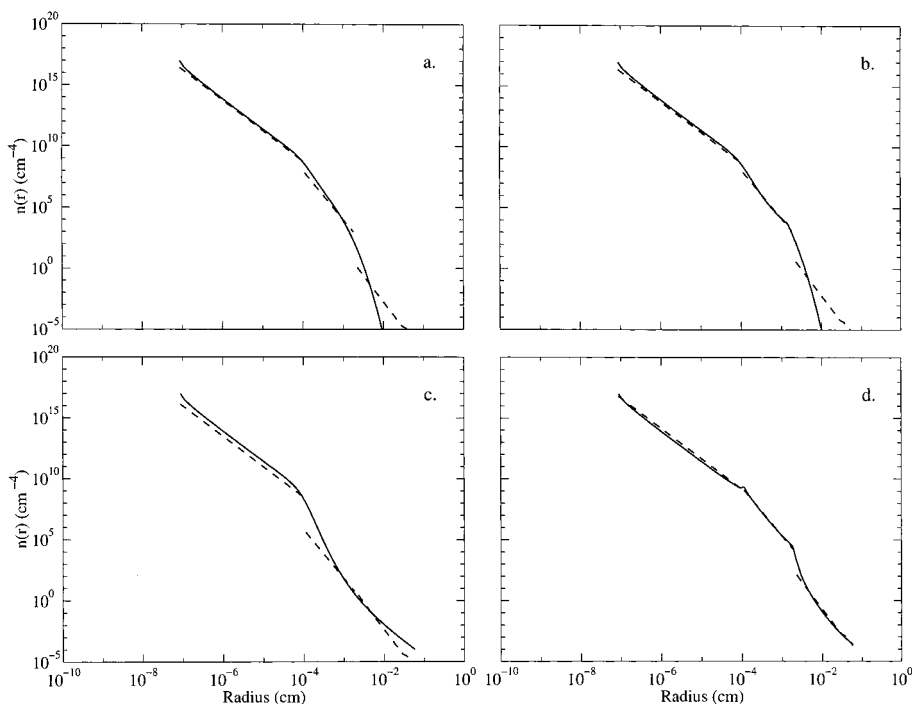


FIGURE 1. Comparison of the modeled steady-state particle size spectrum (solid line) with slopes for the size spectrum calculated using eqs 1–3. The different panels show the effects on the modeled size spectrum when assumptions i–iii in the text are imposed: (a) no additional assumptions, (b) only particles larger than  $40\ \mu\text{m}$  sinking out of the system, (c) no particles in the simulation sink out, and (d) no particle sinking and only one coagulation mechanism operates in each size range.

designed to deal with stiff systems (40) until a steady state was reached.

For the simulations shown here, the monomer density was  $1.2\ \text{g cm}^{-3}$ , the shear was  $\gamma = 0.1\ \text{s}^{-1}$ , the depth of the water was 10 m, the fractal dimension was  $D = 3$ , and the stickiness  $\alpha = 1$ . We chose to show results for  $D = 3$  since our expectation was that this would be case where the two methods would agree the best. Simulations (not shown here) were run for varying parameter values but produced qualitatively the same results.

## Results

The numerically derived steady-state particle size spectrum shows three distinct regions (Figure 1). For particles less than about  $1\ \mu\text{m}$  in radius, the size spectrum has a constant negative slope. In this region of the size spectrum, Brownian motion is the dominant mechanism bringing particles together, and particle settling is negligible because of the small excess densities of the particles. The slope of the size spectrum steepens as the particle radius increases to between 1 and  $10\ \mu\text{m}$ . In this second region, shear is the dominant aggregating mechanism, and some of the larger particles have sufficient settling velocities to sink out of the mixed layer. For particles larger than about  $10\ \mu\text{m}$ , differential sedimentation leads to significant steepening of the size spectrum.

Apart from in the Brownian region ( $r < 1\ \mu\text{m}$ ), the slopes of the size spectrum predicted using eqs 1–3 do not match those resulting from the numerical solution of eq 4 (Figure 1 and Table 1). The results of running the numerical model imposing each of the assumptions enumerated in the Introduction are shown in Figure 1.

The results of assuming that only particles large enough to be dominated by differential sedimentation can settle are shown in Figure 1b. The slopes of the numerically computed size spectrum agree with those calculated from eqs 1–3 in the Brownian and shear regions. However, for the larger

TABLE 1. Comparison of Particle Size Spectrum Slopes in Figure 1<sup>a</sup>

	Brownian	shear	diff. sed.
standard (Figure 1a)	-2.5 (-2.5)	-5.0 (-4.0)	-14.5 (-4.5)
min. size for settling (Figure 1b)	-2.5 (-2.5)	-4.3 (-4.0)	-14.9 (-4.5)
no settling (Figure 1c)	-2.5 (-2.5)	-6.3 (-4.0)	-2.9 (-4.5)
no settling, 1 mechanism per size range (Figure 1d)	-2.5 (-2.5)	-4.0 (-4.0)	-4.6 (-4.5)

<sup>a</sup> Fitted slopes for the numerically calculated size spectra are shown with those calculated from eqs 1–3 in parentheses.

particles, the numerical model predicts a far steeper slope than one would calculate from dimensional analysis.

If we assume that only particles greater than the largest size used in the simulation can settle, then the slope in the differential sedimentation region of the size spectrum is flatter (Figure 1c, note the change in axis). However, in the shear region, the model predicts a steeper slope than that obtained from the dimensional analysis. If in addition we assume that only one aggregation mechanism operates in each size range, then the slopes of the particle size spectrum computed from the numerical model agree with those calculated using dimensional analysis (Figure 1d).

The disaggregation model used has a profound effect on the particle size spectrum (Figure 2), changing  $n(r)$  from a power law to a distinctly bimodal distribution. As expected, disaggregation decreased the particle concentration for the largest particles ( $r > 40\ \mu\text{m}$ ). In addition, the slope of the spectrum for particles with  $r < 0.1\ \mu\text{m}$  was increased. These results strongly conflict with the slopes predicted by the dimensional analysis.

## Discussion

The slopes of the steady-state particle size spectra generated numerically disagree with those given in eqs 2 and 3. The

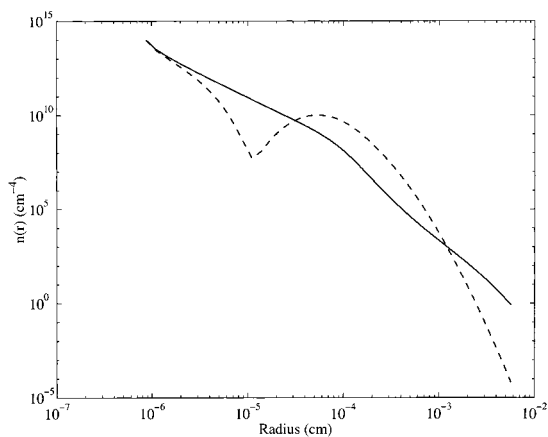


FIGURE 2. Comparison of the calculated steady-state particle size spectrum including disaggregation (dashed line) and without disaggregation (solid line).

differences between the two methods arise not from the assumption of steady state but rather from the ancillary assumptions made in the dimensional analysis. This indicates that caution should be exercised when estimating aggregate properties using eqs 2 and 3.

The shape of the particle size spectrum results from an interplay between several competing mechanisms; particle creation, coagulation, sinking, and disaggregation. In natural systems, these mechanisms all operate over a range of particle sizes. For example, large particles that coagulate predominantly via differential sedimentation also sink, some of them quite rapidly. Predicting the steady-state shape of a particle size spectrum or inferring properties of the particles from the slope of the spectrum requires balancing all these processes for each particle size class.

The simulations presented here were made using rectilinear coagulation kernels. These are the simplest formulations to use, but they neglect the effects of fluid interactions between the particles as well as electrostatic and other forces on the particles (41). These interactions can be incorporated into curvilinear kernel formulations (32). A large particle falling through the water column has to push water from out in front of it as it moves. Smaller particles in the fall line of the larger one follow the fluid streamlines and can get carried far enough away from the larger particle to avoid collision. This interaction affects collisions arising from shear and differential sedimentation and reduces the collision rate of the particles. The result of this is that particles have a greater probability of settling out of the system before aggregating to larger sizes; there are less large particles if curvilinear kernels are used. Consequently, the particle size spectrum using a curvilinear coagulation kernel would be steepened for particle size greater than about 1  $\mu\text{m}$ .

In the absence of disaggregation, there are two mechanisms by which particles can leave the size domain of the model. First, since they can sink, they can settle out of the mixed layer. Alternatively, if the mixed layer is sufficiently deep and the particle sinking rate sufficiently low, the particles can aggregate forming particles larger than the size range being considered. If one stops one of these mechanisms, for example, by assuming that only particles larger than those being considered can settle, then one will increase the number of large particles in the system (Figure 1b,c).

In general, the coagulation eq 4 admits no analytical solutions (12). Consequently, developing approximate solutions and behaviors is an invaluable exercise. For particles with  $r < 1 \mu\text{m}$ , the assumptions used in the dimensional analysis arguments hold to a good degree of approximation (Figure 1); however, in marine systems, particle size spectra

below 1  $\mu\text{m}$  are seldom measured. Particles in this size range are aggregated out of the size range most rapidly by Brownian motion. Natural, colloidal sized particles settle very slowly, far slower than the rates of aggregation of these particles (3). Some of these particles will interact with larger particles via differential sedimentation, but these latter particles are sufficiently rare that they do not cause a significant reduction in the concentration of colloids.

For particles larger than about 1  $\mu\text{m}$ , some of the assumptions listed in the Introduction do not hold. Consider, for example, those particles that aggregate predominantly via differential sedimentation. In order for steady-state conditions to hold, the rates at which particles of a given size are created must balance those removing particles of that size, either through forming larger particles or by removing the particles from the system altogether (17). Balancing settling losses and differential sedimentation introduces the thickness of the water column  $Z$  into the analysis. For large values of  $Z$  and small settling velocities of large particles, particles can have the opportunity to aggregate further. In such cases, the assumptions underlying the dimensional analysis may hold. But for rapidly settling particles, such as fecal pellets, this may not be the case.

Incorporating the assumption that only one aggregation mechanism operates in each size range introduces sharp transitions in the particle size spectrum (Figure 1c) because the rates of aggregation either side of the division are not equal. The result is either an accumulation or relative deficit of particles at the transition size.

Disaggregation is an additional mechanism that can affect the shape of steady-state particle spectra. Aggregation works in one direction, always moving material into larger size classes until the particles are large enough to settle out of the system. Disaggregation works in the opposite direction, creating smaller particles and thereby keeping material in the system for a longer time.

Incorporating disaggregation into the numerical simulation results in a profound change in the particle size spectrum since it affects not only the size spectrum for the larger particles but also smaller particles that would normally only be affected by Brownian coagulation. Fragmentation of larger particles increases the number concentration of particles between about 1 and 10  $\mu\text{m}$ . Because these smaller particles sink slowly, they are removed at a slower rate. The increased numbers of these particles leads to a decrease in the submicron sized particles through coagulation. The movement of mass to particles in the 1–10  $\mu\text{m}$  range creates a maximum in the particle size spectrum there and a local minimum in the size spectrum in the submicron range. This has the effect of steepening the particle size spectrum for large and small particles.

Including disaggregation impedes the continual formation of larger particles, effectively forming a "wall" in the particle size spectrum. In this sense, disaggregation acts rather like a snow fence, forcing material to accumulate in a certain particle size range and preventing the cascade of particles from smaller to ever increasing sizes. Larger particles have a high probability of getting broken up before they are able to settle out of the system, and the accumulation of material in a particular size range increases the rate of aggregation from smaller particles. The size range where material accumulates will depend on a balance between rates of aggregation and disaggregation; in this simulation, the balance is achieved for particles with  $r \sim 1 \mu\text{m}$ .

The shape of the particle size spectrum now arises from a balance between coagulation, settling, and disaggregation. Disaggregation allows for material lost from one particle size class to be introduced into a wide range of smaller size classes. In other words, it allows for the immediate redistribution of material between widely separated size classes without

passing through intermediate classes. For example, particles may be reintroduced into the submicron size range from the breakup of particles larger than 100  $\mu\text{m}$ . What happens at  $\sim 1 \mu\text{m}$  in the Brownian region is directly affected by mechanisms operating in the size range dominated by differential sedimentation. This re-distribution of material is nonlocal in that particles enter a given size class from much larger size classes. This strongly impacts the assumptions used in the dimensional analysis approach.

The disaggregation model that we used was a relatively simple one, with daughter particles being distributed uniformly over all sections smaller than that of the parent particle. More complex models (35–38) distribute the daughter particles nonuniformly. This will have a more complex effect on the shape on the steady-state spectrum.

### Acknowledgments

This work has been funded by grants from the NSF JGOFS/Synthesis and Modeling Program, OCE 97260771 and OCE 9986765. The authors thank Jim Morgan, Charlie O'Melia, and Werner Stumm for their inspiration and guidance on matters aggregate.

### Literature Cited

- (1) O'Melia, C. R. In *Chemical Processes in Lakes*; Stumm, W., Ed.; Wiley: New York, 1985; Chapter 10.
- (2) Farley, K. J.; Morel, F. M. M. *Environ. Sci. Technol.* **1986**, *20*, 187.
- (3) McCave, I. N. *Deep-Sea Res.* **1984**, *31*, 329.
- (4) Hunt, J. R. In *Particulates in Water*; Kavanaugh, M. C., Leckie, J. O., Eds.; American Chemical Society: Washington, DC, 1980; pp 243–257.
- (5) Jiang, Q.; Logan, B. *Environ. Sci. Technol.* **1991**, *25*, 2031.
- (6) Li, X. Y.; Logan, B. E. *Deep-Sea Res. Part II* **1995**, *42*, 125.
- (7) Jackson, G. A.; Lochmann, S. *Limnol. Oceanogr.* **1992**, *37*, 77.
- (8) Honeyman, B. D.; Santschi, P. H. *J. Mar. Res.* **1992**, *47*, 951.
- (9) Burd, A. B.; Moran, S. B.; Jackson, G. A. *Deep-Sea Res.* **2000**, *47*, 103.
- (10) Liyuan, L.; Morgan, J. J. *ACS Sym. Ser.* **1990**, No. 416, 293.
- (11) Liang, L.; Morgan, J. J. *Aquat. Sci.* **1990**, *52*, 32.
- (12) Drake, R. L. In *Topics in Current Aerosol Research*; Hidy, G. M., Brock, J. R., Eds.; Pergamon: New York, 1972; pp 201–377.
- (13) Friedlander, S. K. *J. Meteorol.* **1960**, *17*, 373.
- (14) Friedlander, S. K. *J. Meteorol.* **1960**, *17*, 479.
- (15) Swift, D. L.; Friedlander, S. K. *J. Colloid Interface Sci.* **1960**, *17*, 479.
- (16) Friedlander, S. K.; Wang, C. S. *J. Colloid Interface Sci.* **1966**, *22*, 126.
- (17) Jeffrey, D. J. *J. Atmos. Sci.* **1982**, *38*, 2440.
- (18) van Dongen, D. J.; Ernst, M. H. *Phys. Rev. Lett.* **1984**, *54*, 1396.
- (19) Graham, S. C.; Robinson, A. *J. Aerosol Sci.* **1975**, *7*, 261.
- (20) Meesters, A.; Ernst, M. H. *J. Colloid Interface Sci.* **1987**, *119*, 576.
- (21) Vemury, S.; Pratsinis, S. E. *J. Aerosol Sci.* **1995**, *26*, 175.
- (22) Grant, S. B.; Poor, C.; Relle, S. *Colloids Surf. A* **1996**, *107*, 155.
- (23) Meakin, P. *Fractals, Scaling and Growth Far from Equilibrium*; Cambridge University Press: Cambridge, England, 1998.
- (24) Jackson, G. A.; Maffione, R.; Costello, D. K.; Alldredge, A. L.; Logan, B. E.; Dam, H. G. *Deep-Sea Res.* **1997**, *44*, 1739.
- (25) Wu, M. K.; Friedlander, S. K. *J. Aerosol Sci.* **1993**, *24*, 273.
- (26) Burd, A. B.; Jackson, G. A. *J. Geophys. Res.* **1997**, *102*, 10545.
- (27) Farley, K. J. Ph.D. Dissertation, MIT, 1984.
- (28) Logan, B. E.; Wilkinson, D. B. *Limnol. Oceanogr.* **1990**, *35*, 130.
- (29) Jackson, G. A.; Logan, B. E.; Alldredge, A. L.; Dam, H. G. *Deep-Sea Res. Part II* **1995**, *42*, 139.
- (30) Jackson, G. A. *Deep-Sea Res.* **1995**, *42*, 159.
- (31) Hansen, S.; Ottino, J. M. *Phys. Rev.* **1996**, *E53*, 4209.
- (32) Pruppacher, H. R.; Klett, J. D. *Microphysics of Clouds and Precipitation*; D. Reidel: New York, 1980.
- (33) Vicsek, T. *Fractal Growth Phenomena*, 2nd ed.; World Scientific: Singapore, 1992.
- (34) Parker, D. S.; Kaufman, W. J.; Jenkins, D. J. *San. Eng. Div., Proc. Am. Soc. Civ. Eng.* **1972**, *98*, 79.
- (35) Pandya, J. D.; Spielman, L. A. *J. Colloid Interface Sci.* **1982**, *90*, 517.
- (36) Hill, P. S. *Deep-Sea Res.* **1996**, *43*, 517.
- (37) Kramer, T. A.; Clark, M. M. *J. Colloid Interface Sci.* **1999**, *216*, 116.
- (38) Kramer, T. A.; Clark, M. M. *J. Colloid Interface Sci.* **2000**, *227*, 251.
- (39) Gelbard, F.; Tambour, Y.; Seinfeld, J. H. *J. Colloid Interface Sci.* **1980**, *76*, 541.
- (40) Press, W. H.; Teukolsky, S. A.; Vetterling, W. T.; Flannery, B. P. *Numerical Recipes in FORTRAN: The Art of Scientific Computing*; Cambridge University Press: Cambridge, 1992.
- (41) Israelachvili, J. *Intermolecular and Surface Forces*, 2nd ed.; Academic Press: New York, 1997.

Received for review May 17, 2001. Revised manuscript received September 18, 2001. Accepted October 18, 2001.

ES010982N